

A Sparse Representation Method for Magnetic Resonance Spectroscopy Quantification

Yu Guo, Su Ruan*, Jérôme Landré, and Jean-Marc Constans

Abstract—In this paper, a sparse representation method is proposed for magnetic resonance spectroscopy (MRS) quantification. An observed MR spectrum is composed of a set of metabolic spectra of interest, a baseline and a noise. To separate the spectra of interest, the *a priori* knowledge about these spectra, such as signal models, the peak frequencies, and linewidth ranges of different resonances, is first integrated to construct a dictionary. The separation of the spectra of interest is then performed by using a pursuit algorithm to find their sparse representations with respect to the dictionary. For the challenging baseline problem, a wavelet filter is proposed to filter the smooth and broad components of both the observed spectra and the basis functions in the dictionary. The computation of sparse representation can then be carried out by using the remaining data. Simulation results show the good performance of this wavelet filtering-based strategy in separating the overlapping components between the baselines and the spectra of interest, when no appropriate model function for the baseline is available. Quantifications of *in vivo* brain MR spectra from tumor patients in different stages of progression demonstrate the effectiveness of the proposed method.

Index Terms—Magnetic resonance spectroscopy (MRS) quantification, pursuit algorithm, sparse representation, wavelet filter.

I. INTRODUCTION

MAGNETIC resonance spectroscopy (MRS) has proven clearly to be an important noninvasive tool in biomedical research to study humans and animals [1]. Each biomedical metabolite is identified by its unique position or chemical shift along the frequency axis of an MR spectrum, and the peak intensity or the area under the peak is proportional to the concentration of this assigned metabolite [2]. By accurately quantifying MR spectra (computing the intensities and areas of spectral peaks), the biochemical quantities (concentration) of metabolites can be obtained with some relaxation time corrections, which will not be discussed in detail here.

Manuscript received September 14, 2009; revised January 9, 2010; accepted February 23, 2010. Date of publication May 17, 2010; date of current version June 16, 2010. Asterisk indicates corresponding author.

Y. Guo and J. Landré are with the Centre de Recherche en Sciences et Technologies de l'Information et de la Communication, Université de Reims Champagne-Ardenne, Troyes 10000, France (e-mail: yu.guo@etudiant.univ-reims.fr; jerome.landre@univ-reims.fr).

*S. Ruan is with the Centre de Recherche en Sciences et Technologies de l'Information et de la Communication, Université de Reims Champagne-Ardenne, IUT de Troyes, Troyes 10000, France (e-mail: su.ruan@univ-reims.fr).

J.-M. Constans is with CHU de Caen, Unité d'IRM, Caen cedex 14033, France (e-mail: constans-jm@chu-caen.fr).

Color versions of one or more of the figures in this paper are available online at <http://ieeexplore.ieee.org>.

Digital Object Identifier 10.1109/TBME.2010.2045123

Generally, an observed *in vivo* MR spectrum is composed of many spectra corresponding to different metabolites in a studied region, a large background component mainly originating from macromolecules and lipids, and some noise. For achieving accurate MRS quantification, it is necessary to extract the spectra of individual metabolites from the observed MR spectrum. However, because of the limitation of the signal acquisition system, such as only a single spectrum acquired from one volume element (voxel), poor knowledge about background components, severely overlapping of spectral profiles, and low SNR, the extraction is still a difficult task.

Many MRS quantification methods have been proposed [3]. They can be divided into the following two groups. The first group of MRS quantification methods applies numbers of parameter estimation algorithms to estimate the model parameters of individual resonances in MR spectra, such as VARPRO [4], AMARES [5] in time domain, the method in [6], the circle-fitting (CFIT) method [7] in frequency domain, and the singular value decomposition (SVD) based techniques [8], [9]. The second group of MRS quantification methods, such as LCModel [10], QUEST [11], [12], and AQSES [13], uses metabolite profiles, rather than individual resonances to incorporate maximum information and uniqueness into the analysis, and then, nonlinear optimization algorithms to account for differences between *in vitro* and *in vivo* spectra, and estimate metabolite concentrations. However, it is generally difficult to obtain accurate metabolite profiles, which are significantly important in this group of methods.

A challenging problem in MRS quantification is to remove the large uncharacterized background component, usually called baseline, in an observed MR spectrum, because its presence severely hampers the accuracy of MRS quantifications. In literature, numerous strategies have been proposed to solve the baseline problem [12]. Some of them use some mathematical functions to model baselines [14], [15]. As we cannot know the exact behavior of baselines, these methods could result in estimation errors. Other researchers try to remove baselines with a filter [6] and use the remaining signals for quantifications. However, a portion of useful signals would be also removed after the filtering, which also leads to estimation errors.

In this paper, we propose a frequency-domain MR spectral processing method using sparse representation and a wavelet filter. A preliminary version of this paper has been reported in [16]. In this method, individual resonances of interest are estimated by using a linear pursuit algorithm to find their sparse representations with respect to a dictionary, which is designed based on the mathematical model of MR spectra and the *a priori* knowledge about model parameters. A wavelet filter is used to

filter not only the observed spectrum, but also the basis functions in the dictionary. In this way, this method can finally reconstruct the part of spectrum of interest, which is lost when the baseline is withdrawn. Due to its good performance on both the spectral fitting and the baseline removal, the proposed method can result in an improved MRS quantification, compared to other methods, as shown in this paper.

This paper is organized as follows. We first present the basic theory about sparse representation and the signal model used in this paper. The dictionary construction and the pursuit algorithm employed to find sparse representations are then described in Section II-C and II-D, respectively. The strategy of using a wavelet filter to confront the challenging baseline problem is presented in Section II-E. The evaluation of the proposed method and some quantification results of *in vivo* brain MR spectra are shown in Sections III and IV, respectively. Finally, some discussion and future works are presented.

II. THEORY AND METHOD

A. Sparse Representation

Sparse representation has been attracting more and more interest in the signal processing field in recent years. It is widely used for denoising [17], signal separation [18], direction-of-arrival estimation (DOA) [19], compressed sensing [20], etc. A basic sparse representation model can be described as follows:

$$\mathbf{y} = \mathbf{D}\mathbf{w} \quad (1)$$

where $\mathbf{y}_{N \times 1}$ is a signal vector, which can be sparsely represented as a linear combination of columns (often called “basis vectors”) of a dictionary matrix $\mathbf{D}_{N \times M} = [\mathbf{d}_1, \mathbf{d}_2, \dots, \mathbf{d}_M]$, and when $M > N$, it is an overcomplete dictionary. $\mathbf{w}_{M \times 1}$ is the representation coefficient vector, minimal elements of which are nonzero.

In the research of sparse representation, activity has concentrated on the construction of dictionaries and the study of pursuit algorithms computing sparse signal representation with respect to a given dictionary. The dictionaries should be designed to better fit the model in (1), and generally, designing dictionaries can be done by either selecting one from a prespecified set of linear transforms or adapting the dictionary to a set of training signals [21]. In our method, the constructed dictionary is prespecified based on the signal model and some *a priori* knowledge that will be described in the next section.

Theoretically, the sparsest representation of a signal vector \mathbf{y} with respect to a given dictionary \mathbf{D} is equivalent to the following optimization problem:

$$\min_{\mathbf{w}} \|\mathbf{w}\|_0 \text{ subject to } \mathbf{y} = \mathbf{D}\mathbf{w} \text{ or } \|\mathbf{y} - \mathbf{D}\mathbf{w}\|_2 \leq \varepsilon \quad (2)$$

where $\|\cdot\|_0$ is l_0 norm to count the nonzero entries of a vector and ε is a parameter specifying how much noise we wish to allow. However, it is an nondeterministic polynomial time (NP) hard problem, which means that the time required to solve the problem using any currently known algorithm increases very quickly as the size of the problem grows. Thus, greedy methods and approximate solution methods based on convex relaxations are proposed in literature and these methods can yield maximally

sparse representations under certain conditions. The matching pursuit (MP) [22] and the orthogonal least square (OLS) [23] algorithms are the most commonly used greedy algorithms to compute sparse representations. A greedy algorithm selects basis functions sequentially, following some rules, such as involving the computation of inner products between the signal and dictionary columns in the MP algorithm. Some other methods use approximate solutions, such as minimizing l_1 -norm by the basis pursuit algorithm [17], l_p -norm ($1 \leq p \leq 2$) by the iterative reweighted-based algorithms [19], [24], or a smooth function by the smooth l_0 -norm algorithm [25] to replace the minimization of l_0 -norm in (2). For these approximate solution methods, the problem is that the solutions are not sufficiently sparse due to the convexification of the true sparsity measure. In our paper, a pursuit algorithm based on focal underdetermined system solver (FOCUSS) is developed and applied.

B. Signal Model

Generally, an observed MR spectrum \mathbf{x} can be modeled as follows:

$$\mathbf{x} = \mathbf{S} + \mathbf{B} + \mathbf{e} = \sum_{k=1}^K \mathbf{s}_k + \mathbf{B} + \mathbf{e} \quad (3)$$

where \mathbf{S} represents the mixed metabolite spectrum of interest, \mathbf{B} is a baseline contribution, \mathbf{e} is Gaussian noise, and \mathbf{s}_k is the lineshape function of the k th resonance. A Lorentzian lineshape in (4) or a Gaussian lineshape in (5) or the combination of Lorentzian and Gaussian lineshapes are usually used for the approximation of \mathbf{s}_k

$$L_k(f) = \frac{a_k}{1 + [(f - f_k)/d_k]^2} \quad (4)$$

$$G_k(f) = a_k \exp \left[- \left(\frac{f - f_k}{d_k} \right)^2 \right] \quad (5)$$

where f is the frequency of each data point, a_k is the amplitude, d_k is the linewidth, and f_k is the peak frequency of the resonance \mathbf{s}_k [6]. a_k, f_k, d_k ($k = 1, \dots, K$) are model parameters estimated in most MRS quantification methods, such as the methods in [4]–[7]. The specific relative frequencies of resonances, or their chemical shifts, are normally used to identify the biochemical species from which these resonances originate and are considered constant in most situations, where they are used as *a priori* knowledge to improve the estimation of other spectral parameters [1].

C. Dictionary Construction

With the signal model of MR spectra taken into consideration, the direct method to estimate each resonance is nonlinear parameter estimation algorithms. In our method, by constructing a dictionary, we attempt to solve the problem by employing a linear sparse representation estimation algorithm. Finally, the resonances of interest \mathbf{s}_k ($k = 1, \dots, K$) in (3) are estimated by finding their sparse representations in the constructed dictionary.

Due to the fact that the resonances of interest can be linearly represented by Gaussian and Lorentzian functions, and

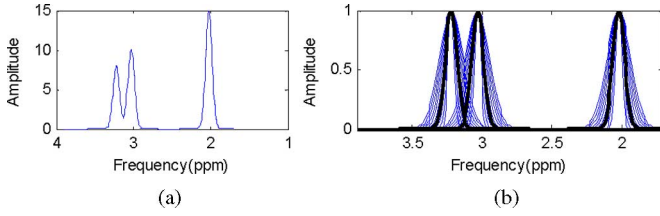


Fig. 1. Illustration of the dictionary construction. (a) Simulated MR spectrum with three peaks (simulated with Gaussian functions). (b) Normalized Gaussian basis functions in the corresponding dictionary [the black lines represent the best approximations of the three spectral peaks in (a)].

different resonances have different peak frequencies, we construct a dictionary, which is composed of a set of normalized Gaussian and Lorentzian functions, as shown in (4) and (5). The *a priori* knowledge about peak frequencies and the range of possible linewidths of each resonance are used to fix parameters of these basis functions. In this way, the constructed dictionary will contain as few basis functions as possible, while still representing the resonances of interest very well.

For each basis function in the dictionary, its central frequency is set as the known peak frequency of a certain resonance f_k ($k = 1, \dots, K$). For the basis functions with the same central frequency, their linewidths d_k change in a given range with a certain sampling interval. According to central frequencies, the dictionary is divided into K groups $\{D_1, D_2, \dots, D_k, \dots, D_K\}$, where K is the number of possible resonances in a mixed MR spectrum. Basis functions $\{d_{k1}, \dots, d_{kj}, \dots, d_{kL}\}$ in the group D_k have the same central frequency f_k and different linewidths denoted as $d_{kj} = d_{k1} + (j-1)\Delta d_k$ ($j = 1, \dots, L$), where L is the number of basis functions in the group, $[d_{k1}, d_{kL}]$ is the range of possible linewidth of the resonance s_k and Δd_k is the sampling interval.

Different groups can have different numbers of basis functions. Here for convenience, we assume the same number of basis functions in different groups. When the range of the possible linewidths of the resonance s_k is determined, the choice of Δd_k will decide the number of basis functions L in the group D_k . The relatively small value of Δd_k will lead to more accurate representations of resonances, but stronger correlations between basis functions, which will make it difficult to accurately estimate sparse representation in the next step. For the choice of the sample step Δd_k , there has to be a compromise between robustness and precision.

Fig. 1 shows a simulated MR spectrum with three spectrum peaks and the corresponding basis functions in a dictionary to represent the spectrum. The black lines in Fig. 1(b) correspond to the basis functions, which can best approximate the three spectrum peaks in Fig. 1(a). The objective of our method is to search the three basis functions.

The constructed dictionary is denoted as a matrix with M basis vectors $\{d_1, d_2, \dots, d_i, \dots, d_M\}$, where $M = K \times L$. If the sparse representation vector of a mixed spectrum S is denoted as w , then

$$S = Dw = \sum_{i=1}^M d_i w_i = \sum_{k=1}^K D_k w_k \quad (6)$$

where $w = [w_1^T, w_2^T, \dots, w_k^T, \dots, w_K^T]^T$. Theoretically, only the basis functions, which best approximate the resonances of interest correspond to nonzero representation coefficients. In the case, where different resonances have different peak frequencies, the basis vectors in group D_k can only represent the resonance s_k . Therefore, there is $s_k = D_k w_k$. Let $\hat{w} ([\hat{w}_1^T, \hat{w}_2^T, \dots, \hat{w}_k^T, \dots, \hat{w}_K^T]^T)$ denote the estimated sparse representation of a mixed spectrum, the resonance s_k can be estimated as $\hat{s}_k = D_k \hat{w}_k$.

D. Pursuit Algorithm

To estimate the sparse representations of MR spectra with respect to the constructed dictionary, some points should be considered. Firstly, because basis functions in the same group have the same central frequency, strong correlations exist between them. Therefore, the pursuit algorithms, such as the MP and the basis pursuit, which have severe restriction on the correlations between basis functions, will perform poorly here. Secondly, the intensity of each resonance is, in general, nonnegative and the expected representation coefficients will also be nonnegative, therefore, nonnegative constraint can be added. Taking these into account, we develop an algorithm based on the FOCUSS method in [19] and [24] to estimate the sparse representation in (6).

The FOCUSS method proposed in [19] minimizes the $l_{(p \leq 1)}$ diversity measure $E^{(p)}(w)$ to replace l_0 -norm in (2) and ensure sparsity

$$E^{(p)}(w) = \sum_{i=1}^M \text{sgn}(p) |w(i)|^p \quad (7)$$

where $p < 1$. Then, the approximate sparse representation becomes the solution of

$$\min_w E^{(p)}(w) \text{ subject to } y = Dw. \quad (8)$$

Concerning noise in the measurements, a Bayesian framework is used in [24]. w is estimated by using a MAP estimator defined as follows:

$$w = \arg \min_w J(w), \text{ where} \\ J(w) = [\|Dw - y\|^2 + \gamma E^{(p)}(w)] \quad (9)$$

The parameter γ controls the compromise between the quality of fitting y and the degree of sparsity. A larger value of γ leads to sparser solutions, and a smaller value leads to better fit.

When w has nonnegative properties, this constraint should be added to the optimization as shown in the following equation:

$$w = \arg \min_w J(w), \\ \text{where } J(w) = [\|Dw - y\|^2 + \gamma E^{(p)}(w)] \text{ and } \forall i : w_i \geq 0. \quad (10)$$

Here, based on the basic iterative form of the regularized FOCUSS algorithm in [24] for finding the sparse solution of

(9), an iterative form for (10) is proposed as follows:

$$\begin{aligned} 1) \quad & \mathbf{w}_{k+1} = \mathbf{W}_{k+1} \mathbf{D}_{k+1}^T (\mathbf{D}_{k+1} \mathbf{D}_{k+1}^T + \lambda \mathbf{I})^{-1} \mathbf{y} \\ 2) \quad & w_{k+1}(i) = \begin{cases} 0, & \text{if } w_{k+1}(i) < 0 \\ w_{k+1}(i), & \text{if } w_{k+1}(i) \geq 0 \end{cases} \end{aligned}$$

where $\mathbf{W}_{k+1} = \text{diag}(|w_k(1)|^{1-(p/2)}, \dots, |w_k(M)|^{1-(p/2)})$ and $\mathbf{D}_{k+1} = \mathbf{D} \mathbf{W}_{k+1}$. At each iteration step, the negative values of the updated solution \mathbf{w}_{k+1} are set to zero to ensure the nonnegativity of \mathbf{w} . Actually, the nonnegativity constraint also increases the sparsity of a solution to a certain degree. The regularization parameter λ is the function of the level of noise. In [24], three different criteria for choosing λ are investigated. They are 1) quality of fit; 2) a sparsity criterion; and 3) L -curve. Here, for the consideration of computational efficiency, λ is set as $C\varepsilon^2$, where ε is the estimated noise power and C is a constant chosen by a thorough analysis of simulated data.

E. Baseline Removal

In frequency domain, baselines are commonly assumed to be smooth and broad compared to the resonance signals. This assumption can be used to remove the baselines from spectral signals by applying a wavelet filter [6], [26] or by modeling the baselines [27]. In this paper, a new strategy is proposed. First, a wavelet filter is used to remove the smooth components of an observed spectrum in which there is not only the baseline, but also a portion of useful signal. The signal remaining after the filtering consists of only a component of mixed resonances of interest, which does not overlap with the baseline. Our idea is to carry out the estimation of sparse representation on the remaining signal to finally reconstruct the resonances of interest in their entirety.

A wavelet filter is denoted as $g(\bullet)$. $\mathbf{x}_h = g(\mathbf{x})$ is the result of filtering an observed spectrum \mathbf{x} with $g(\bullet)$. $\mathbf{x}_l = \mathbf{x} - \mathbf{x}_h$ is the smooth component removed by the filter. Because of the overlapping of \mathbf{B} and \mathbf{s}_k ($k = 1, \dots, K$), when the baseline \mathbf{B} is eliminated completely by the wavelet filter, the smooth and broad components of metabolite spectra will also be lost at the same time. This can be denoted as: $\mathbf{x}_h \approx \mathbf{S}_h$ and $\mathbf{x}_l \approx \mathbf{B} + \mathbf{S}_l$, where $\mathbf{S}_h = g(\mathbf{S})$ and $\mathbf{S}_l = \mathbf{S} - \mathbf{S}_h$. To represent \mathbf{S}_h , all the basis vectors $\{\mathbf{d}_1, \mathbf{d}_2, \dots, \mathbf{d}_M\}$ in the dictionary \mathbf{D} analyzed in Section II-C are also processed by the same wavelet filter. A new dictionary \mathbf{D}_h using the remaining components $g(\mathbf{d}_i)$ ($i = 1, \dots, M$) is then constructed. The signal \mathbf{x}_h remaining after filtering can be written as follows:

$$\mathbf{x}_h = \mathbf{S}_h + \xi_B = \mathbf{D}_h \mathbf{w} + \xi_B \approx \mathbf{D}_h \mathbf{w} \quad (11)$$

where ξ_B is the remaining component of the baseline after the wavelet filtering, which should be as small as possible. Finally, the representation coefficient vector \mathbf{w} of mixed resonances \mathbf{S} with respect to the dictionary matrix \mathbf{D} in (6) can be estimated by computing the sparsest solution of (11).

In our paper, a wavelet filter with discrete Coiflet mother wavelet, which can result in a good fitting with the smooth baseline is used [26]. The choice of the level of the wavelet decomposition is made dependent on the smoothness of baselines. It needs to be emphasized that if too much component of

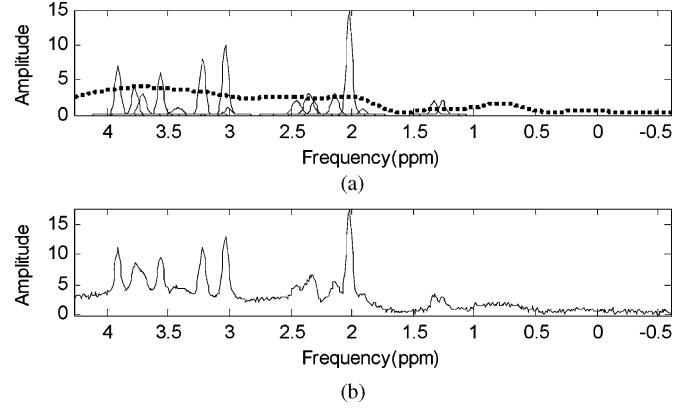


Fig. 2. Simulated ^1H human brain MR spectra. (a) Simulated resonances (solid lines) and baseline (dotted line). (b) Simulated observed spectrum (SNR = 18 dB and SBR = 0 dB).

TABLE I
PARAMETERS OF THE SIMULATED ^1H MR SPECTRA

Metabolite	k^h	f_k (ppm)	d_k (ppm)	a_k
Cr	1	3.91	0.03	7.00
Glu/Gln 1	2	3.77	0.03	4.00
Glu/Gln 2	3	3.71	0.04	3.00
mI	4	3.56	0.03	6.00
Tau	5	3.42	0.06	1.00
Cho	6	3.22	0.03	8.00
Cr/PCr	7	3.03	0.03	10.00
GABA 1	8	3.01	0.03	1.00
GABA 2	9	2.31	0.03	2.00
GABA 3	10	1.91	0.03	1.00
Glu/Gln 3	11	2.45	0.05	2.00
Glu/Gln 4	12	2.35	0.05	3.00
Glu/Gln 5	13	2.14	0.04	3.00
NAA	14	2.02	0.03	15.00
Lac1	15	1.33	0.03	2.00
Lac2	16	1.26	0.03	2.00

an observed MR spectrum is removed by the wavelet filter, the remaining component \mathbf{S}_h will not contain enough information to reconstruct \mathbf{S} .

III. EVALUATION AND RESULTS

The proposed method is first evaluated by using both simulated ^1H and ^{31}P human brain MRS data. The objective of our paper is to provide an automatic tool for followup of changes in MR quantification of patients during therapeutic treatment. The proposed method has been tested on *in vivo* MRS data of six patients, who benefit from MRS examinations every 3 to 6 months.

A. Simulated ^1H Human Brain MR Spectra

1) *Simulated Data*: First, simulated ^1H human brain MR spectra are used to evaluate our method. A simulated spectrum with 512 data points contains 16 resonances, a baseline and a Gaussian noise. Each resonance is simulated as a Gaussian function, as shown in Fig. 2(a). The parameters of these functions are summarized in Table I. The simulated baseline in Fig. 2(a) is obtained from a similar baseline of a true ^1H human brain MR spectrum.

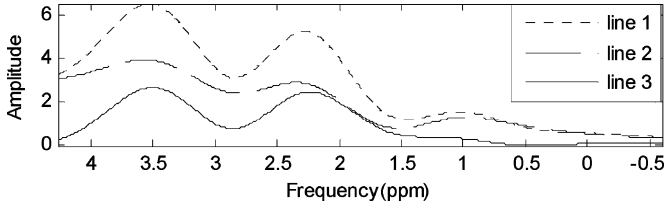


Fig. 3. Removed components from Fig. 2(b) with the wavelet filter in our paper. The total removed component (line 1), which is the sum of the removed resonance component (line 2) and the removed baseline component (line 3).

To test the robustness of different methods under different baseline and noise conditions, a number of observed spectra with different SNR (12, 14, 16, 18, and 20 dB) and signal-to-baseline ratios (SBR = -4, -2, 0, 2, and 4 dB) are simulated. Here, SNR is defined as the ratio of the highest amplitude of these simulated resonances to the noise standard deviation and SBR is the power ratio of a mixed spectrum of interest to the simulated baseline. For a given baseline and noise condition, a set of 100 observed MR spectra is generated in order to give reliable estimation results and to check the robustness of different methods. Fig. 2(b) shows a simulated observed spectrum with SNR = 18 dB and SBR = 0 dB.

In simulation experiments, as an *a priori* knowledge, basis functions in the constructed dictionary have the known central frequencies as the parameters f_k ($k = 1, \dots, 16$) listed in Table I and the unknown linewidths taken from the range $0.01 \leq d \leq 0.10$ ppm with a sample step $\Delta d = 0.002$ ppm.

The wavelet filter used to remove baselines performs a 5-level wavelet decomposition [Coiflet wavelet (COIF5)] of the observed MR spectra. The detail coefficients of wavelet decompositions are retained to construct x_h . The same wavelet decomposition and reconstruction of each basis vector in D is computed to construct a new dictionary D_h . In the simulation experiments, the regularization parameter λ of the proposed pursuit algorithm is set as $C\epsilon^2$ and $C = 0.4$.

Fig. 3 shows the removed components of the observed spectrum in Fig. 2. We can observe that when most baseline components are removed by the filter, a few resonance components are also removed. We can also see that the baseline is not completely removed. However, due to the robustness of the proposed pursuit algorithm, the residual portion of the baseline does not significantly influence the estimation of representation coefficients. Additionally, if more components are filtered, despite the fact that no component of baseline is left, too many resonance components will be removed, leading to the lack of information for the accurate estimation of the expected representation coefficients.

2) Results on Simulated Data: In simulation experiments, the proposed method is compared with another frequency-domain MRS quantification method proposed in [6]. The method in [6], which is called nonlinear method in this paper, uses the Levenberg–Marquardt algorithm to estimate the nonlinear model parameters of metabolite spectra and a wavelet filter to remove the baseline component in an iterative subtraction manner. The quantification results of the two methods in

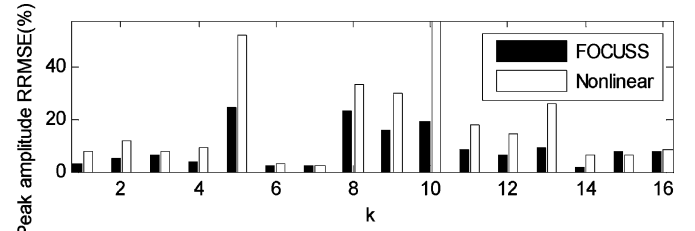


Fig. 4. Statistic quantification results for the simulated resonances in Fig. 2(a) (SNR = 18 dB and SBR = 0 dB) with two methods: the proposed method and the nonlinear method.

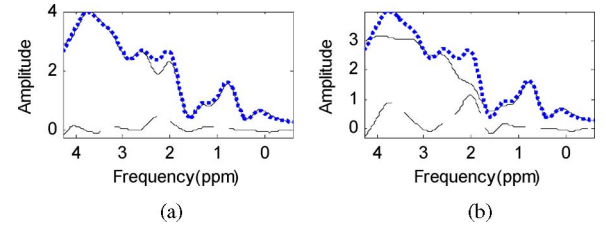


Fig. 5. Estimated baselines in a simulation experiment (SNR = 18 dB and SBR = 0 dB) with two methods (dotted lines: simulated baseline, solid lines: estimated baseline, and dashed line: estimation errors). (a) Proposed method. (b) Nonlinear method.

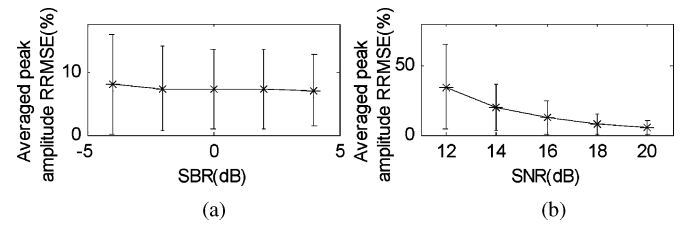


Fig. 6. Means and standard deviations of peak amplitude RRMSEs of all the resonances in Fig. 2 under different baseline and noise conditions. (a) SBR = -4, -2, 0, 2, and 4 dB, and SNR = 18 dB. (b) SNR = 12, 14, 16, 18, and 20 dB and SBR = 0 dB.

100 simulation experiments (SNR = 18 dB and SBR = 0 dB) are compared. The relative root mean square error (RRMSEs) of estimated peak amplitudes are given in Fig. 4. The RRMSE is defined as the ratio of RMSE of estimated results to the real values. Fig. 5 shows the estimated baselines with the two methods in one experiment. As observed in Figs. 4 and 5, the proposed method has better quantification accuracy compared with the nonlinear method in [6]. For the metabolites with weak MRS peaks, such as the metabolites Tau ($k = 5$) and GABA ($k = 8, 9, 10$), the proposed method can provide much better quantifications than the method in [6].

In our paper, we also analyze the quantification performance of the proposed method under different noise and baseline conditions. The means and standard deviations of peak amplitude RRMSEs of all resonances are calculated. Fig. 6(a) shows the results under a given noise condition (SNR = 18 dB) and different baseline conditions (SBR = -4, -2, 0, 2, and 4 dB). Because most of baseline components have been filtered by the wavelet filter and the few residual baseline components limit the influence of the amplitude change of baselines on the final estimation accuracy, the estimation results of the proposed

TABLE II
PARAMETERS OF THE SIMULATED ^{31}P MR SPECTRA AND BASELINE (THE COMBINATION OF THREE LORENTZIAN FUNCTIONS)

	Spectra											Baseline		
k	1	2	3	4	5	6	7	8	9	10	11	1	2	3
f_k (Hz)	-86	-70	-54	152	168	292	308	360	440	490	530	-800	200	800
d_k (Hz)	50	50	50	50	50	50	50	25	285.7	25	200	2500	3000	2500
a_k	4.5	9.0	4.5	9.0	9.0	9.0	9.0	18.0	14.6	7.2	7.5	3.2	3.4	5.3

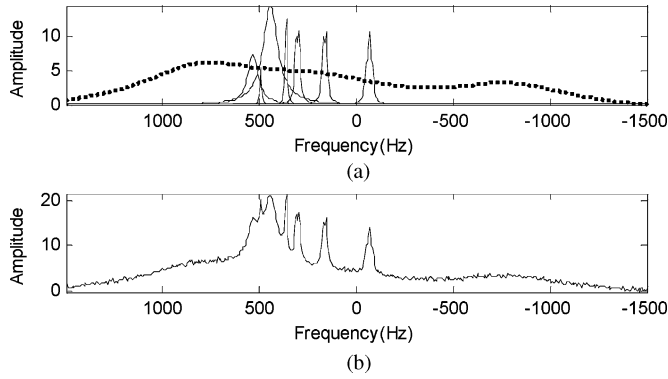


Fig. 7. Simulated ^{31}P human brain MR spectra. (a) Simulated resonances (solid lines) and baseline (dotted line). (b) Simulated observed spectrum (SNR = 18 dB and SBR = 0 dB).

method change little with the increase in baseline amplitude. Fig. 6(b) shows the results under a given baseline condition (SBR = 0 dB) and different noise conditions (SNR = 12, 14, 16, 18, and 20 dB). It can be seen that when the level of noise increases, estimation results deteriorate as with most other MRS quantification methods and noise has more important influence on the quantification of small peaks than on that of large peaks.

B. Simulated ^{31}P Human Brain MR Spectra

1) *Simulated Data:* ^{31}P human brain MR spectra are also simulated to evaluate the proposed method. A simulated ^{31}P human brain MR spectrum with 512 data points is composed of 11 resonances, a baseline and a Gaussian noise. Each resonance is simulated as a Lorentzian function and the baseline is simulated as the sum of three Lorentzian functions. The parameters of simulated resonances and baseline are summarized in Table II (f_k : frequency, d_k : linewidth, and a_k : amplitude). Fig. 7(a) shows the plots of 11 simulated resonances and the simulated baseline. Fig. 7(b) shows a simulated observed spectrum with SNR = 18 dB and SBR = 0 dB.

Different from the experiments with simulated ^1H MRS data, besides the *a priori* knowledge about central frequencies, the *a priori* knowledge of adenosine triphosphate (ATP) doublets (α -ATP and γ -ATP peaks) and triplet (β -ATP peaks) used in [7] and [9] is also integrated into the dictionary construction in our method. For the triplet peaks, they have the same linewidth ($d_1 = d_2 = d_3$) and their amplitudes have the relation $a_1 = a_2/2 = a_3$. For the doublet peaks, they have the same linewidths ($d_4 = d_5$; $d_6 = d_7$) and amplitudes ($a_4 = a_5$; $a_6 = a_7$). Making use of this *a priori* knowledge, we include the basis functions in the dictionary, consisting of a combination of several Lorentzian functions satisfying the aforementioned constraints to represent the doublet or triplet peaks. The linewidths of all the Lorentzian

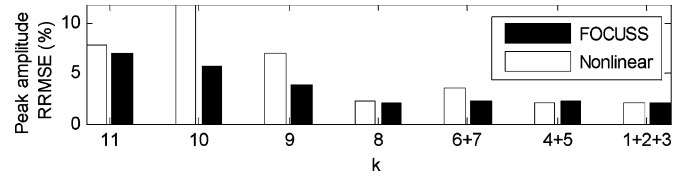


Fig. 8. Quantification results for the simulated resonances in Fig. 8 (SNR = 18 dB and SBR = 0 dB) with two methods: the proposed method and the nonlinear method.

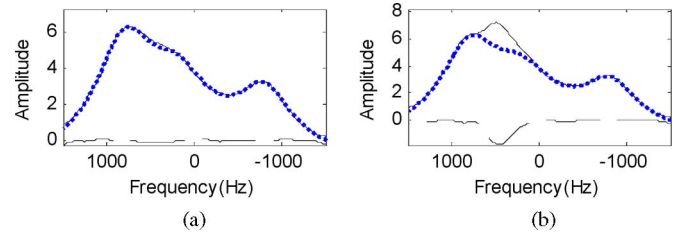


Fig. 9. Estimated baselines in a simulation experiment (SNR = 18 dB and SBR = 0 dB) with two methods taking into account broad components and lipids (dotted lines: simulated baseline, solid lines: estimated baseline, and dashed line: estimation errors). (a) Proposed method. (b) Nonlinear method.

TABLE III
QUANTIFICATION RESULTS OF A PATIENT WITH TIME IN TWO REGIONS: TUMOR REGION (ZONE 1) AND NORMAL REGION (ZONE 2)

Region and time	NAA/Cr	Cho/Cr	mI/Cr
Zone1 date: 2006-12-09	1.0767	1.2930	1.2149
Zone2 date: 2006-12-09	1.6548	0.8296	0.6036
Zone1 date: 2007-06-20	1.3022	1.1325	1.1125
Zone2 date: 2007-06-20	1.7019	0.8957	0.6658
Zone1 date: 2007-11-22	1.2654	1.3288	1.4344
Zone2 date: 2007-11-22	1.5489	1.3732	1.1583

functions used to construct the dictionary are taken from the range $10 \leq d \leq 400$ Hz with a sample $\Delta d = 10$ Hz. In addition, the same wavelet filter as that used for simulated ^1H MRS data is applied to remove baselines.

2) *Results on Simulated Data:* The comparison between our proposed method and the nonlinear method in [6] was also carried out on simulated ^{31}P MR spectra with SNR = 18 dB and SBR = 0 dB in Fig. 7. The same *a priori* knowledge was used in both methods. The quantification results (RRMSEs of estimated peak amplitudes) for the two methods in 100 simulation experiments are given in Fig. 8, which shows better performance with the proposed method. In Fig. 8, we can see that for the resonances ($k = 9, 10, 11$), which seriously overlap with the baseline, the nonlinear method cannot give accurate quantification results. Fig. 9 shows the estimated baselines obtained by

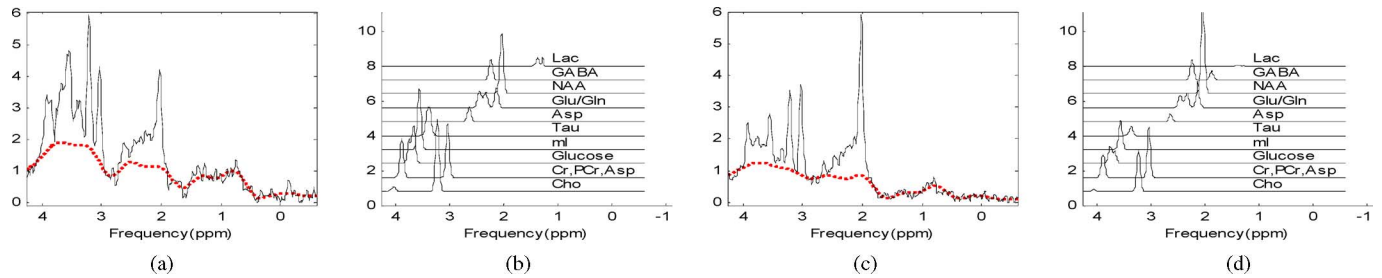


Fig. 10. Separation results of *in vivo* spectra with the acquisition time 09-2-2006. (a) Observed spectrum (OS) from tumor tissue (zone 1) and the estimated baseline (dotted line). (b) Estimated resonances with the spectrum in (a). (c) OS from normal tissue in the contralateral hemisphere (zone 2) and the estimated baseline (dotted line). (d) Estimated resonances with the spectrum in (c).

the two methods in one experiment, respectively. It is obvious that the nonlinear method cannot separate the baseline and the spectrum of interest when there is an overlap between these two elements, and thus, gives poor baseline estimation. By contrast, the proposed method can estimate the baseline very well.

Moreover, the simulated ^{31}P MR spectrum shown in Fig. 7 is also quantified with the “advanced magnetic resonance (AMARES) routine” method in magnetic resonance user interface (MRUI) package [28], which is based on the nonlinear optimization method proposed in [5] and commonly used in the MRS quantification field. In the “AMARES routine”, the presence of baselines in MR spectra is not considered, therefore, we first used the baseline correction tool in the MRUI to remove baselines, and then, the “AMARES routine” to fit spectra of interest. The *a priori* knowledge was also incorporated in the “AMARES routine” as in the proposed method. For the three β -ATP peaks, the estimations were totally wrong. The average relative estimation error of the other eight peak amplitudes was 51%. However, if no baseline presents in the simulated spectrum, the average relative estimation error of the 11 peak amplitudes is only 4.64%, which is considered as good performance. This shows that the great quantification errors of the spectra with baseline derive from the unsuccessful baseline removal. As is known, baselines are always present in MR spectra and pose a severe quantification problem. Therefore, it is important for an MRS quantification technique to have good performances on both the spectral fitting and the baseline removal.

IV. MRS QUANTIFICATION IN HUMAN BRAIN TUMORS INFOLLOW-UP

The proposed method is used to quantify *in vivo* ^1H human brain MR spectra of six patients with brain lesions. MR spectra are recorded for these patients every six months at 1.5T with point-resolved spectroscopy (PRESS) and with an echo-time of 35 ms in two opposite regions in their brains. The two regions chosen by the doctor correspond to one region with tumor (zone 1) and one presumed normal brain region (zone 2) in the contralateral hemisphere, respectively. The estimated peak amplitude ratios of three metabolites [*N*-acetylaspartate (NAA), choline-containing compounds (Cho), myo-inositol (mI)] to the metabolite canrenone (Cr) are calculated at each MRS examination to show the progression. Results of one patient are illustrated in Table III, showing quantitative information about the

tumor. Fig. 10 shows two observed spectra of a patient recorded at the same time from zone 1 and zone 2, respectively, as well as their corresponding spectral separation results.

As expected, NAA/Cr is decreased in the tumor zone, while Cho/Cr, mI/Cr, and lactate/Cr are increased. Large variations in mI/Cr due to water suppression, coupling, baseline, or multiple instrumental parameters remain. It is also observed from Table III that the proposed method is able to detect spectral and metabolic changes under patient treatment even in the contralateral side (zone 2), for example, the small spectral variations between 09-12-2006 and 20-06-2007 mainly due to instrumental, normal biological variation, and some variation under chemotherapy, and that between 20-06-2007 and 22-11-2007 either due to beginning of treatment effect or beginning of infiltration or glycolytic metabolism. In the tumor side (zone 1), this method is also capable of detecting a good initial response to patient treatment between 09-12-2006 and 20-06-2007 and a glial reaction despite the diversification instrumental, which is not always easy to detect, for example, small lactate changes (witness of early metabolic switch spontaneously or under therapy). The quantification results of these spectra can help doctors to diagnose tumors and analyze the progression of the metabolite components of brain tumors at different therapy stages.

For the processing of the *in vivo* MR spectra with 512 sample points, it takes on average 3.12 ± 0.3 s with implementation on a PC (AMD Core processor 2.0 GHz and 2 GB of memory) using the MATLAB v 7.1 under Microsoft Windows XP.

V. CONCLUSION

In this paper, we have presented a novel frequency-domain spectral analysis technique, which uses sparse representation and wavelet filtering to separate baselines and the resonances of interest in MR spectra. The proposed method can accurately estimate the resonances of interest by finding their sparse representations without the perturbation caused by baselines. Simulation experiments show its superiors for separating the overlapping components of the baselines and the spectra of interest, compared with other methods.

In addition, in our paper, the *a priori* knowledge about the peak frequencies are used to reduce computational complexity and improve the quantification performance for overlapping peaks. Furthermore, in the case of small changes in peak

frequencies, our method can adapt to the problem by modifying the dictionary.

In future works, this method will be tested on a large number of *in vivo* MRS data to construct dictionaries, which can adapt to and represent various types of MR spectra. By analyzing the characteristics of baselines in detail, we will be able to develop an autoadaptable method for choosing wavelet filter parameters for resolving baseline problems. The signal characteristics caused by sideband artefacts, hidden peaks, asymmetric line-shape, and uneven phasing should be studied more extensively on a much larger database and could be handled in preprocessing steps, and/or changing and improving basis functions in the constructed dictionary.

REFERENCES

- [1] H. J. A. in't Zandt, M. van der Graaf, and A. Heerschap, "Common processing of *in vivo* MR spectra," *NMR Biomed.*, vol. 14, pp. 224–232, Jun. 2001.
- [2] J. A. Stanley, J. W. Pettegrew, and M. S. Keshavan, "Magnetic resonance spectroscopy in schizophrenia: Methodological issues and findings. Part I," *Soc. Biol. Psychiatry*, vol. 48, pp. 369–380, Sep. 2000.
- [3] J. B. Pouillet, D. M. Sima, and S. Van Huffel, "MRS signal quantitation: A review of time- and frequency-domain methods," *J. Magn. Reson.*, vol. 195, pp. 134–144, Sep. 2008.
- [4] J. W. van der Veen, R. de Beer, P. R. Luyten, and D. van Ormondt, "Accurate quantification of *in vivo* ^{31}P NMR signals using the variable projection method and prior knowledge," *Magn. Reson. Med.*, vol. 6, pp. 92–98, Jan. 1988.
- [5] L. Vanhamme, A. van den Boogaart, and S. Van Huffel, "Improved method for accurate and efficient quantification of MRS data with use of prior knowledge," *J. Magn. Reson.*, vol. 129, pp. 35–43, Nov. 1997.
- [6] P. Gillies, I. Marshall, M. Asplund, P. Winkler, and J. Higinbotham, "Quantification of MRS data in the frequency domain using a wavelet filter: An approximated Voigt lineshape model and prior knowledge," *NMR Biomed.*, vol. 19, pp. 617–626, Jun. 2006.
- [7] R. E. Gabr, R. Ouwerkerk, and P. A. Bottomley, "Quantifying *in vivo* MR spectra with circles," *J. Magn. Reson.*, vol. 179, pp. 152–163, Mar. 2006.
- [8] N. Sandgren, Y. Selen, P. Stoica, and J. Li, "Parametric methods for frequency selective MR spectroscopy—A review," *J. Magn. Reson.*, vol. 168, pp. 259–272, Jun. 2004.
- [9] P. Stoica, Y. Selen, N. Sandgren, and S. Van Huffel, "Using prior knowledge in SVD-based parameter estimation for magnetic resonance spectroscopy—the ATP example," *IEEE Trans. Biomed. Eng.*, vol. 51, no. 9, pp. 1568–1578, Sep. 2004.
- [10] S. W. Provencher, "Estimation of metabolite concentrations from localized *in vivo* proton NMR spectra," *Magn. Reson. Med.*, vol. 30, pp. 672–679, Dec. 1993.
- [11] H. Ratiney, F. Mitri, Y. Coenradie, S. Cavassila, D. van Ormondt, and D. Graveron-Demilly, "Quest: Time-domain quantitation with advanced prior knowledge," in *Proc. 19th Annu. Meet., Eur. Soc. Magn. Reson. Med. Biol.*, Cannes, France, Nov. 2002, p. 373.
- [12] H. Ratiney, M. Sdika, and Y. Coenradie, "Time-domain semiparametric estimation based on a metabolite basis set," *NMR Biomed.*, vol. 18, pp. 1–13, Jan. 2005.
- [13] J. Pouillet, D. M. Sima, A. W. Simonetti, B. D. Neuter, L. Vanhamme, P. Lemmerling, and S. Van Huffel, "An automated quantitation of short echo time MRS spectra in an open source software environment: AQSES," *NMR Biomed.*, vol. 20, pp. 493–504, Dec. 2006.
- [14] L. Hofmann, J. Slotboom, C. Boesch, and R. Kreis, "Characterization of the macromolecular baseline in localized ^1H -MR spectra of human brain," *Magn. Reson. Med.*, vol. 39, pp. 855–863, Oct. 2001.
- [15] J. A. Stanley and J. W. Pettegrew, "Postprocessing method to segregate and quantify the broad components underlying the phosphodiester spectral region of *in vivo* ^{31}P brain spectra," *Magn. Reson. Med.*, vol. 45, pp. 390–396, Feb. 2001.
- [16] Y. Guo, S. Ruan, J. Landré, and J.-M. Constans, "A Priori knowledge-based frequency domain quantification of magnetic resonance spectroscopy," presented at the 7th IFAC Symp. Model. Control Biomed. Syst., Aalborg, Denmark, Aug. 2009.
- [17] S. S. Chen, D. L. Donoho, and M. A. Saunders, "Atomic decomposition by basis pursuit," *SIAM J. Sci. Comput.*, vol. 20, pp. 33–61, 1999.
- [18] Y. Li, S. Amari, A. Cichocki, D. W. C. Ho, and S. Xie, "Underdetermined blind source separation based on sparse representation," *IEEE Trans. Signal Process.*, vol. 54, no. 2, pp. 423–437, Feb. 2006.
- [19] I. F. Gorodnitsky and B. D. Rao, "Sparse signal reconstruction from limited data using FOCUSS: A reweighted norm minimization algorithm," *IEEE Trans. Signal Process.*, vol. 45, no. 3, pp. 600–616, Mar. 1997.
- [20] D. L. Donoho, "Compressed sensing," *IEEE Trans. Inf. Theory*, vol. 52, no. 4, pp. 1289–1306, Apr. 2006.
- [21] A. Michal, E. Michael, and B. Alfred, "K-SVD: An algorithm for designing overcomplete dictionaries for sparse representation," *IEEE Trans. Signal Process.*, vol. 54, no. 11, pp. 4311–4322, Nov. 2006.
- [22] S. Mallat and Z. Zhang, "Matching pursuits with time-frequency dictionaries," *IEEE Trans. Signal Process.*, vol. 41, no. 12, pp. 3397–3415, Dec. 1993.
- [23] S. Chen, S. A. Billings, and W. Luo, "Orthogonal least squares methods and their application to non-linear system identification," *Int. J. Control*, vol. 50, pp. 1873–1896, 1989.
- [24] B. D. Rao, K. Engan, S. F. Cotter, J. Palmer, and K. Kreutz-Delgado, "Subset selection in noise based on diversity measure minimization," *IEEE Trans. Signal Process.*, vol. 51, no. 3, pp. 760–770, Mar. 2003.
- [25] H. Mohimani, M. Babaie-Zadeh, and M. Jutten, "A fast approach for overcomplete sparse decomposition based on smoothed ℓ_0 norm," *IEEE Trans. Signal Process.*, vol. 57, no. 1, pp. 289–301, Jan. 2009.
- [26] K. Young, V. Govindaraju, B. J. Soher, and A. A. Maudsley, "Automated spectral analysis II: Application of wavelet shrinkage for characterization of non-parameterized signals," *Magn. Reson. Med.*, vol. 40, pp. 816–821, Dec. 1998.
- [27] B. J. Soher, K. Young, and A. A. Maudsley, "Representation of strong baseline contributions in ^1H MR spectra," *Magn. Reson. Med.*, vol. 45, pp. 966–972, May 2001.
- [28] A. Naressi, C. Couturier, J. M. Devos, M. Janssen, C. Mangeat, R. de Beer, and D. Graveron-Demilly, "Java-based graphical user interface for the MRUI quantitation package," *Magn. Reson. Mater. Phys., Biol. Med.*, vol. 12, pp. 141–152, Jun. 2001.

Yu Guo received the B.S. and M.S. degrees in electronic engineering from Dalian University of Technology, Dalian, China, in 2005 and 2007, respectively. She is currently working toward the Ph.D. degree in Centre de Recherche en Sciences et Technologies de l'Information et de la Communication, University of Reims Champagne-Ardenne, Troyes, France.

Her current research interests include statistical signal processing and sparse representation with application to signal separation.

Su Ruan received the Ph.D. degree in image processing from the University of Rennes 1, Rennes, France, in 1993.

From 1993 to 2003, she was an Associate Professor at the University of Caen, Caen, France. Since 2003, she has been with the Centre de Recherche en Sciences et Technologies de l'Information et de la Communication, University of Reims Champagne-Ardenne, Troyes, France, where she is currently a Full Professor. Her research interests include image segmentation, data fusion and pattern recognition, and medical image processing.

Jérôme Landré was born in France in 1972. He received the Ph.D. degree in image indexing from the University of Burgundy, Dijon, France, in 2005.

He was a Computer Science Engineer at the University of Burgundy, for ten years. Since 2008, he has been with the University of Reims Champagne-Ardenne, Troyes, France, where he is currently an Assistant Professor. His research interests include signal and image processing using wavelets and sparse representations.

Jean-Marc Constans received the Ph.D. degree from the University of Caen Basse-Normandie, Caen, France, in 2006.

He was a Maître de Conférences Universitaire and a Praticien Hospitalier with the University of California, San Francisco and VA Medical Center San Francisco, CA, for three years, where he was engaged in research in magnetic resonance (MR), especially in spectroscopy. Since 1993, he has been with the University Hospital of Caen, Caen, France. His current research interests include development, evaluation, and application of MR techniques and methods in segmentation and in proton spectroscopy on brain diseases.